


*Communication*

# 3D Printing of Functional Assemblies with Integrated Polymer-Bonded Magnets Demonstrated with a Prototype of a Rotary Blood Pump

Kai von Petersdorff-Campen <sup>1,\*</sup>, Yannick Hauswirth <sup>1</sup>, Julia Carpenter <sup>2</sup>, Andreas Hagmann <sup>3</sup>, Stefan Boës <sup>1</sup> , Marianne Schmid Daners <sup>1</sup>, Dirk Penner <sup>4</sup> and Mirko Meboldt <sup>1</sup>

<sup>1</sup> Product Development Group Zurich, Department of Mechanical and Process Engineering, ETH Zurich, 8092 Zurich, Switzerland; yannicha@ethz.ch (Y.H.); sboes@ethz.ch (S.B.); marischm@ethz.ch (M.S.D.); meboldtm@ethz.ch (M.M.)

<sup>2</sup> Complex Materials, Department of Materials, ETH Zurich, 8093 Zurich, Switzerland; julia.carpenter@mat.ethz.ch

<sup>3</sup> Arnold Magnetic Technologies AG, 5242 Birr-Lupfig, Switzerland; andreas.hagmann@arnoldmagnetics.ch

<sup>4</sup> Laboratory of Ceramic Materials, Institute of Materials and Process Engineering, ZHAW School of Engineering, 8400 Winterthur, Switzerland; penr@zhaw.ch

\* Correspondence: kaiv@ethz.ch; Tel.: +41-44-63-20176

Received: 15 July 2018; Accepted: 29 July 2018; Published: 1 August 2018



**Featured Application:** 3D printing with a polymer-bonded magnetic filament allows all-in-one print of a functioning prototype of a rotary blood pump.

**Abstract:** Conventional magnet manufacturing is a significant bottleneck in the development processes of products that use magnets, because every design adaption requires production steps with long lead times. Additive manufacturing of magnetic components delivers the opportunity to shift to agile and test-driven development in early prototyping stages, as well as new possibilities for complex designs. In an effort to simplify integration of magnetic components, the current work presents a method to directly print polymer-bonded hard magnets of arbitrary shape into thermoplastic parts by fused deposition modeling. This method was applied to an early prototype design of a rotary blood pump with magnetic bearing and magnetic drive coupling. Thermoplastics were compounded with 56 vol.% isotropic NdFeB powder to manufacture printable filament. With a powder loading of 56 vol.%, remanences of 350 mT and adequate mechanical flexibility for robust processability were achieved. This compound allowed us to print a prototype of a turbodynamic pump with integrated magnets in the impeller and housing in one piece on a low-cost, end-user 3D printer. Then, the magnetic components in the printed pump were fully magnetized in a pulsed Bitter coil. The pump impeller is driven by magnetic coupling to non-printed permanent magnets rotated by a brushless DC motor, resulting in a flow rate of 3 L/min at 1000 rpm. For the first time, an application of combined multi-material and magnet printing by fused deposition modeling was shown. The presented process significantly simplifies the prototyping of products that use magnets, such as rotary blood pumps, and opens the door for more complex and innovative designs. It will also help postpone the shift to conventional manufacturing methods to later phases of the development process.

**Keywords:** 3D printing; rapid prototyping; additive manufacturing; fused deposition modelling; printable magnets; permanent magnets; rotary blood pump

## 1. Introduction

In iterative product development, conventional manufacturing methods with long lead times are a significant bottleneck for fast testing and validation. This holds true especially for the development of products that use magnets, where the fabrication of custom magnet shapes by e.g., sintering, hot-pressing, or injection molding is time- and cost-intensive and requires special tooling [1].

Furthermore, conventional manufacturing techniques restrict the design of new and complex structures, not only for magnets but also in product development, because the assembly steps necessary to integrate the magnets into parts impose restrictions on design and prolong iteration cycles. The use of rapid manufacturing methods for magnets during prototyping phases could, therefore, be of great benefit.

Recently, studies have applied 3D printing techniques to magnetic materials to produce magnets with complex geometries and tailored magnetic fields. Li et al. used pellets of a NdFeB/Nylon compound to print large magnets with a remanence of 510 mT by big area additive manufacturing (BAAM) [2]. Huber et al. used a similar compound to produce filaments with high NdFeB content for printing magnets with a remanence of 314 mT via fused deposition modeling (FDM) [3–5]. While these approaches are based on polymer-bonded magnetic compounds, Jaćimović et al. printed purely metallic magnets by means of selective laser melting of NdFeB powder, reaching the maximum remanence measured in any printed permanent magnet of 590 mT [6]. Further approaches for the additive manufacturing of magnets include binder jetting [7] and direct ink writing [8,9].

With the exception of Li et al. who demonstrated the use of a printed magnet in a conventional DC motor, the translation of 3D printed magnets to actual use cases has not been made [10]. For printing by FDM [3–5], an inhibiting factor might be the reported use of non-optimized injection molding compounds that result in brittle filaments poorly suited for unsupervised handling on conventional FDM printers.

Extensive iterative testing is of critical importance, especially during the development of biomedical devices, to ensure reliable operation and successful approval procedures. Rotary blood pumps (RBPs) are, next to heart transplantation, the only option for patients suffering from end-stage heart failure. Such RBPs have magnets as critical components in the driving and bearing systems of the impeller. RBPs which are currently available have the undesired side effects of hemolysis and thrombus formation that have to be addressed in the design and development phase of next-generation devices [11,12]. Although computational fluid dynamics are often used in the early design stage, validating computational data experimentally is crucial [13]. While standard 3D printing is already partly being applied in RBP development [14–16], to the best of the authors' knowledge, 3D printing of magnets is not yet being used for testing new designs of medical devices.

In this work, a functional pump with a magnetic driving and bearing system is printed in one print to show the feasibility of combining multiple material printing and magnet printing for the rapid development of RBPs. For this purpose, a flexible, highly-loaded magnetic compound filament (MagFil) is developed. This filament can be processed on a low-cost, end-user multi-material FDM printer. The chosen design exploits the designing freedom of additive manufacturing and cannot be manufactured conventionally.

## 2. Materials and Methods

### 2.1. Printing

For the printing process, a low-cost, end-user FDM printer was chosen (Prusa i3 MK2 with a multi-material upgrade, Prusa Research, Prague, Czech Republic). It is capable of printing up to four different thermoplastic filaments in one print. Four Bowden-style dual extruders are attached to the frame of the printer, and flexible tubes guide the filaments from the extruders to a so-called multiplexer on the printer head. The multiplexer joins the four filament channels, leading to a 0.6 mm diameter nozzle. All materials are extruded through the same nozzle. During phases in the print job where a

filament is not used, it is retracted into the multiplexer for solidification. The print bed is coated with a polyetherimide sheet. The empirically-found printing parameters for the developed MagFil material are presented in Table 1. The slicer software, Slic3r Prusa edition 1.39.1 ([www.slic3r.org](http://www.slic3r.org)) was used to generate the machine code for the 3D printer from the 3D model files.

**Table 1.** Empirically-found printer parameters for the developed polymer-bonded compound filament (MagFil).

Parameter	Value
Extruder temperature	220 °C
Layer height	0.15–0.25 mm
Printer speed	25 mm/s
Infill density	100%
Infill pattern	Rectilinear
Bed temperature	60 °C

## 2.2. Filament Materials

A 5-component polymer-bonded magnetic compound was developed for the fabrication of a filament optimized towards a high-powder loading and mechanical flexibility. The components consisted of a magnetically isotropic NdFeB powder, an isotropic NdFeB powder/Polyamide-12 (PA12) compound used in injection molding, polyoxymethylene (POM) as the main matrix material, a dispersing agent, and Aerosil as the rheology optimizing additive. Table 2 gives details on the materials, manufacturers, and the compound composition.

**Table 2.** Composition of the developed flexible polymer-bonded compound filament (MagFil).

Ingredient	Type	Weight Fraction	Volume Fraction
NdFeB powder	MQP-S-11-9 (NdPrFeCoTiZrB), Magnequench (Singapore)	66.03%	42.34%
NdFeB/PA12 compound	BMNPI-60HR, Bomatec (Höri, Switzerland)	24.46%	23.07%
POM	F10-01, Kepital (Wiesbaden, Germany)	7.34%	24.79%
Dispersing agent	Edaplan 935, Münzing (Abstatt, Germany)	1.98%	9.35%
Fumed silica	Aerosil, Evonik (Essen, Germany)	approx. 0.20%	approx. 0.44%
Total magnet powder <sup>1</sup>	-	88.53% <sup>2</sup> / 91.40% <sup>3</sup>	56.19% <sup>2</sup>

<sup>1</sup> The total amount of magnetic particles contributed by NdFeB powder as well as NdFeB/PA12 compound.

<sup>2,3</sup> Calculated from amounts used in the composite according to thermogravimetric analysis (TGA).

The diameter and shape of the NdFeB powder particles (MQP-S-11-9) were given by the manufacturer as spherical with a diameter of  $42 \pm 13 \mu\text{m}$ . The NdFeB/PA12 compound had a specified magnetic powder filling of 60 vol.%. Details on the size and shape of the compounded magnetic particles were not disclosed by the manufacturer. The remanence, intrinsic coercivity, and maximum energy product of the NdFeB powder and NdFeB/PA12 compound are presented in Table 3. Both the NdFeB/PA12 compound and POM were obtained as granules. As both polymers (PA12 and POM) have a high melt flowability with excellent mechanical strength and toughness, they are suited for processing as highly-filled plastics. To further reduce the viscosity of the composite and to ensure a homogeneous particle distribution in the matrix, a high molecular weight-dispersing agent was used. It was further intended to serve as corrosion protection and for mitigating fire risk of the dry NdFeB powder, and was added as 3% of the powder weight. To improve powder flowability and reduce friction between the magnet particles, a small amount of fumed silica was added. Initial experiments revealed that the order of mixing influenced the processability and homogeneity of the compound. The following order proved to be beneficial: First, mixing the NdFeB and fumed silica powders and, separately, the POM granules with the dispersing agent. Then, combining the two mixtures with the NdFeB/PA12 compound granules, for further processing.

**Table 3.** Magnetic properties of the NdFeB powder, the NdFeB/PA12 compound, and the MagFil material.

Parameter	NdFeB Powder	NdFeB/PA12 Compound	MagFil Material
Remanence (mT)	730–760 <sup>1</sup>	515–575 <sup>2</sup>	353 (SD = 6%)
Intrinsic coercivity (kA/m)	670–750 <sup>1</sup>	620–800 <sup>2</sup>	711 (SD = 0.2%)

<sup>1</sup> According to the manufacturer Magnequench, Singapore. <sup>2</sup> According to the manufacturer Bomatec, Höri, Switzerland.

The compounding of the final mixture and filament extrusion was performed on a parallel twin-screw extruder with a nozzle diameter of 2.5 mm (Process 11, ThermoFisher Scientific, Karlsruhe, Germany). The 8 temperature zones (Z) were set with increasing temperatures from 200 °C at the feeder (Z1) to 220 °C at the nozzle (Z8) (Z1/Z2: 200 °C, Z3/Z4: 210 °C, Z5/Z6: 215 °C, Z7/Z8: 220 °C). The extrudate was collected by a conveyer belt and cooled down with an air stream for accelerated solidification. A filament diameter of 1.75 mm was targeted by adjusting the speed of the conveyer belt. Subsequently, the filament was spooled onto a 0.45 m diameter spool using a spooling machine (Belt Take-Off BAW 1300 with Horizontal Winder WR 650, Collin, Ebersberg, Germany) and later transferred to a standard spool with a diameter of 10 cm.

Further materials used for printing of the pump prototype were a polylactide (PLA) filament (PLA silver 1.75 mm, Prusa Research, Prague, Czech Republic) and a butenediol vinyl alcohol copolymer (BVOH) filament (BVOH 1.75 mm, Verbatim, Tokio, Japan).

### 2.3. Magnetization

The printed objects were magnetized with a pulse magnetizer (MC Magnetizer, MAGSYS Magnet Systeme, Dortmund, Germany) using a Bitter electromagnet at Arnold Magnetic Technologies AG (Birr-Lupfig, Switzerland) with a maximum magnetic flux density of 6 T.

### 2.4. Material Characterization

Scanning electron microscopy (LEO 1530, Zeiss, Oberkochen, Germany) images were taken to determine the shape, size, and distribution of NdFeB particles in the polymer matrix. The average particle size was determined by measuring the diameter of 100 particles visible on the fracture surface. To this purpose, a filament was broken manually and the fracture surface coated with 5 nm of Gold (sputter coater, CCU-010, Safematic, Bad Ragaz, Switzerland). The gravimetric fraction of NdFeB particles was determined with thermogravimetric analysis (STA 449C, Netzsch GmbH, Selb, Germany) in an argon atmosphere by heating to 700 °C at 10 °C/min (TGA). The filament density was determined according to Archimedes' principle with water as the immersible phase.

To evaluate the remanence and intrinsic coercivity of printed parts and their variation, the demagnetization curves of 10 printed cylinders ( $\varnothing$  15 mm, h = 5 mm) were measured using a permagraph (Permagraph L, Magnet-Physik, Dr. Steingroever GmbH, Cologne, Germany). Furthermore, the surface roughness of the 10 cylinders was determined using a laser scanning microscope (VK-X260K, Keyence, Neu-Isenburg, Germany). The roughness was determined separately for vertical and horizontal surfaces. Ten profile lines per sample with a length of 700  $\mu$ m were used. The profile lines were aligned parallel to the building direction for vertical surfaces and angularly distributed for horizontal surfaces.

### 2.5. Pump Demonstrator Design and Testing

The basic design of the pump prototype is similar to that of conventional RBP designs—however, complicated geometries with inside twists and undercut elements would not allow for conventional manufacturing. The bearing concept for the impeller consisted of two passive magnetic bearings for radial forces and a pivot tip for axial forces. For the radial magnetic bearings, hollow cylinder magnets

were integrated into the impeller and housing. The impeller comprises of four blades with twisted internal blade channels in a helical shape around the inflow axis (Figure 1a). In each of the blades, a driving magnet was embedded just above the bottom surface. The shape of the magnet was matched to the blade geometry, thereby maximizing the magnet volume (Figure 1b). The impeller was actuated by magnetic coupling to a set of matching non-printed permanent magnets spinning on a servo motor just below the housing.

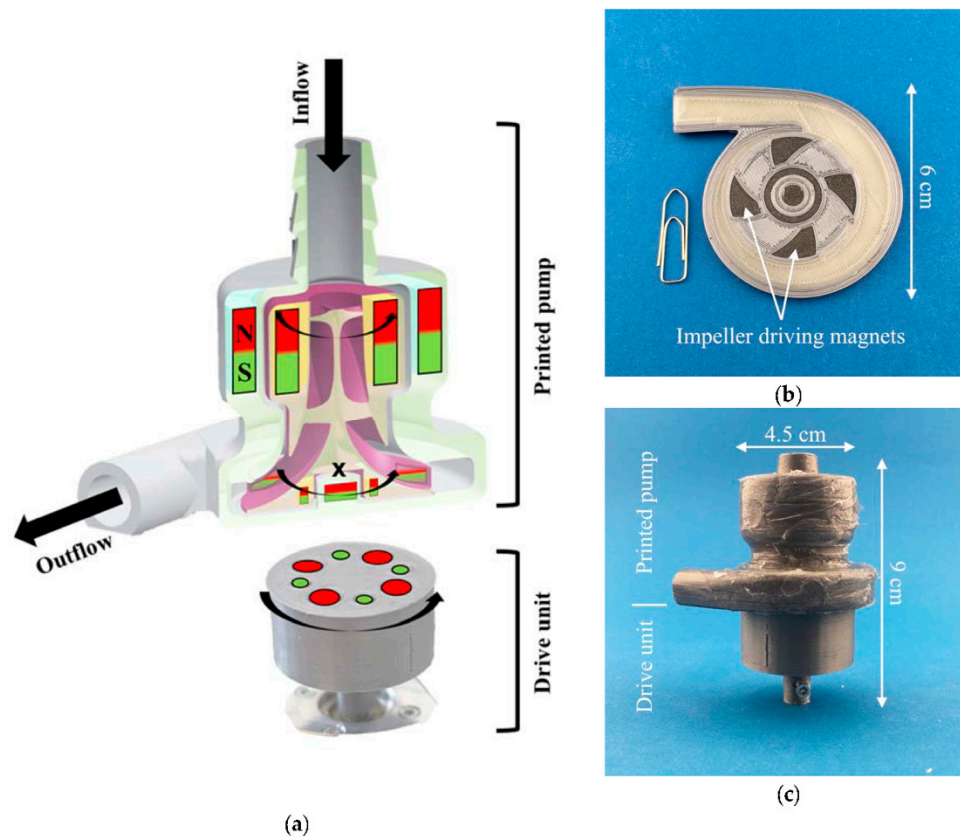


**Figure 1.** (a) Design scheme and coupling of the printed pump with integrated driving and bearing magnets in the housing and impeller; (b) Cross-section of the printed pump showing the used materials in different colors (silver: PLA, black: magnetic compound, beige: water-soluble BVOH); (c) Fully printed pump with drive unit after removal of support material (no magnets visible, coated with silicone).

The housing and the impeller were printed in one single print using three different filament materials. The MagFil filament was used for printing the magnetic components, a PLA filament was used as the building material in which the magnets were embedded, and a BVOH filament as a water-soluble support material to support overhangs during printing and to separate the impeller and housing (Figure 1b, MagFil: black, PLA: silver, BVOH: white). After the magnetization step, the major fraction of the support material was dissolved by placing the entire part in water for several hours. As the support material showed insufficient solubility in small gaps, the pump was cut open and glued back together after removal of residual BVOH. The pump prototype was coated with silicone grease from the outside to prevent leakage during testing.

The hydraulic performance of the pump was tested with water using an ultrasonic flow probe (TS410/ME-11PXL, Transonic Systems, Ithaca, NY, USA) and pressure sensors (MX960, Smiths Medical, Minneapolis, MN, USA) at the pump inlet and outlet.

### 3. Results and Discussion

#### 3.1. Material Characterization

The extruded filament had sufficient flexibility to be spooled to a conventional filament spool with a diameter of 10 cm and could be processed on a Bowden principle FDM printer, in which filaments undergo significant bending. This is an improvement compared to published polyamide-based compositions (PA11 [3,4], PA12 [5]) that yield brittle filaments processable only with large bending radii. Initial experiments with only POM as the matrix phase yielded bendable filaments that were very soft and ground up in the extruder of the printer. The addition of PA12 in the form of a NdFeB/PA12 compound increased the resistibility in the extruder of the printer while simultaneously maintaining sufficient bendability.

A diameter within the range of 1.65 and 1.85 mm complying with the required tolerance could be achieved (Figure 2a). SEM imaging confirmed the expected spherical morphology and close packing of the NdFeB particles (Figure 2b). The average particle size was  $48 \pm 15 \mu\text{m}$ . The residual mass of 91.40 wt.% recorded by TGA analysis was comparable to the amount of filler used in the composite (88.53 wt.%, Table 2), which indicates that compounding was able to provide good dispersion of the filler within the matrix. The comparison between the measured filament density of  $4.27 \text{ g/cm}^3$  with the theoretical value of  $4.78 \text{ g/cm}^3$  indicates a certain amount of porosity (approx.  $P_{\text{filament}} = 10.6 \text{ vol.}\%$ ).

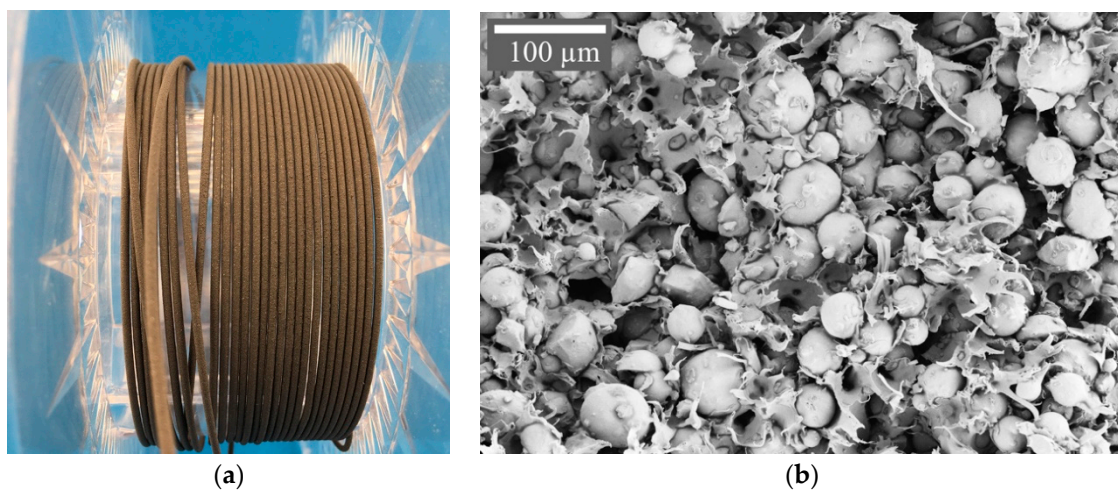


**Figure 2.** (a) Polymer-bonded magnetic filament flexible enough to be spooled on a standard filament spool with a diameter of 10 cm; (b) SEM micrograph of the extruded polymer-bonded magnetic compound, NdFeB particles inside the POM/PA12 matrix.

Printing of precise objects with smooth surfaces was achieved. The minimum feature size determined by the extrusion width of a single printed line was approximately  $500 \mu\text{m}$ . The surface of the printed cylinders was smooth, with an average roughness of  $R_a = 23.7 \mu\text{m}$  ( $SD = 35\%$ ) on vertical surfaces and  $R_a = 12.4 \mu\text{m}$  ( $SD = 17\%$ ) on the top surfaces. This surface roughness is well within the range of reported values for standard plastic FDM parts [17–20]. The cylinder size and shape were very good, in accordance with the corresponding 3D model (on average 3.5% and 2% larger in diameter and height, respectively). From visual comparison with images of various printed magnets published by Huber et al., it is apparent that the achieved surface quality and geometric precision is equal or better to them [3,4]. The density of printed samples  $3.67 \text{ g/cm}^3$  ( $SD = 7\%$ ) indicated a further increase of porosity during printing by approximately 14% to about  $P_{\text{cylinder}} = 24\%$ . This decrease in density due to the printing process was also reported by Huber et al. (15% [5], 22% [3,4]).

The remanence of the printed cylinders was  $B_{r, \text{cylinder}} = 353 \text{ mT}$  ( $SD = 6\%$ ) which is slightly higher than the published values for printable NdFeB compound filaments (314 mT [5] (given), 301 mT [4]

(estimated from given compound remanence and density of printed parts)). A theoretical value  $B_{r, th, dense} = 466$  mT can be calculated under the assumption of a dense composite and a linear relation of the volumetric powder filling with the remanence (analog to Huber et al. [5]). Therefore, the measured remanence of the printed cylinders  $B_{r, cylinder}$  exhibits the same deviation of approximately 24% from the theoretical calculation as the porosity  $P_{cylinder}$ . Hence, it is likely that the decrease in remanence is mainly caused by porosity, and other factors, like oxidation, are insignificant. Figure 3 shows the achieved remanences in the context of conventionally manufactured and 3D printed magnets, as well as theoretical values for the MagFil material based on the volumetric powder filling.

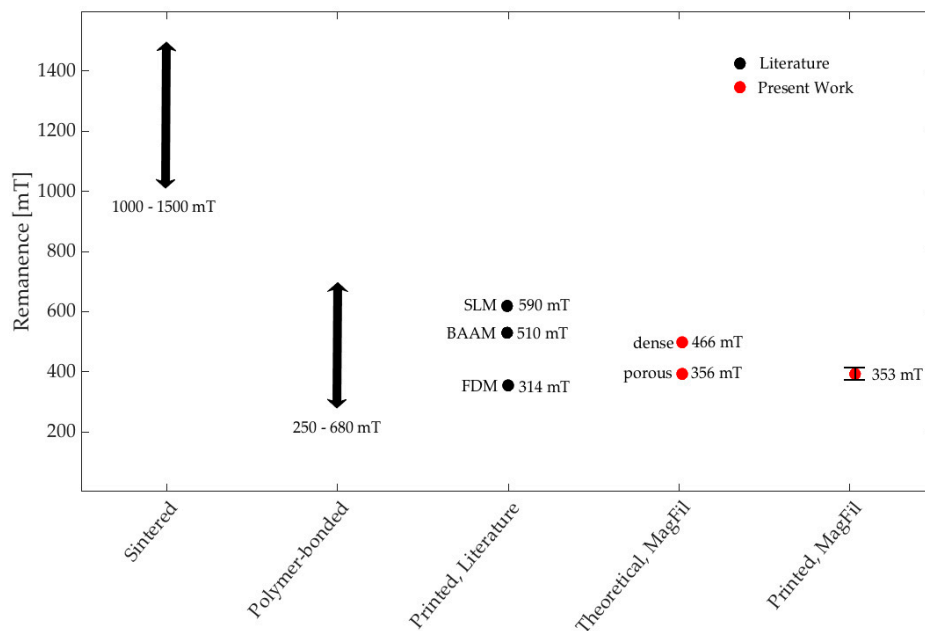


**Figure 3.** Comparison of remanences of NdFeB magnets in the form of commercially available sintered magnets [21], polymer-bonded magnets [22], magnets printed by selective laser melting (SLM) [6], big area additive manufacturing (BAAM) [2], and fused deposition modelling (FDM) [5] (Printed, Literature), theoretical remanences of the developed polymer-bonded magnetic compound as dense material and according for a porosity of 24% (Theoretical, MagFil) and the measured remanence of printed MagFil cylinders (Printed, MagFil; SD = 7%).

The intrinsic coercivity of the printed cylinders was 711 kA/m (SD = 0.2%) and seems to be independent of the volumetric powder filling and the porosity of the printed parts, as this lies within the range of the given values of the magnetic starting materials (Table 3).

### 3.2. Pump Demonstrator Manufacturing and Testing

The aim to fabricate a prototype design of an RBP with magnetic bearing and magnetic drive coupling was achieved. The pump was successfully printed in one print (Figure 1c) with a print time of approximately 15 h and tested after support material removal and silicone coating.

During multiple-material printing, the use of a single-nozzle printer can cause loss of printing precision and process stability. Occasionally, the MagFil filament is ground up in the extruder due to increased stress during filament changes. The necessity to co-print a wipe-tower to clean the nozzle after each filament change drastically increases the printing time. Contamination of the nozzle with the oily dispersing agent from the MagFil material diminishes proper layer adhesion of the concomitantly printed filaments, PLA and BVOH. Furthermore, the feature size for PLA- and BVOH-regions is limited due to the use of a large 0.6 mm diameter nozzle necessary to prevent clogging by NdFeB particles. A simple solution targeting all named problems with low investment costs could be the

use of a multi-nozzle printer that renders filament changes unnecessary and allows use of different nozzle diameters for each material. While this is expected to raise the printing quality to the standard FDM level, the FDM-inherent residual surface roughness will remain, and might limit the range of applicability for the present method.

An operation of the pump prototype at a maximum rotational speed of 1000 rpm, with a flow rate of 3 L/min against a pressure head of 6 mmHg was achieved. At higher rotational speeds, the magnetic coupling broke off and the delivered flow rate decreased concomitantly. The pump prototype could therefore not deliver a sufficient flow rate at head pressures that are realistic for clinically used RBPs. This can be linked to the inferior printing quality caused by the above-described difficulties during multi-material printing. Due to insufficient layer adhesion of the PLA material and subsequent layer delamination, the pump surfaces were rougher and small features less precise compared to usual FDM parts. This caused additional friction and imbalances, for which the strength of the printed magnets was insufficient to compensate. Furthermore, the rough inner surfaces and material choice render hemocompatibility highly unlikely [23].

The presented method allows only one polarization over all magnetic parts of one print, as a demagnetized powder is used during printing and the magnetic parts are magnetized when already embedded. A possible approach is to use already magnetized hard magnetic particles or to magnetize the particles during the printing process. These particles could then be aligned when exiting the nozzle by magnetic fields, as shown by Kim et al., for direct ink writing of magnetic elastomer composites [24].

#### 4. Conclusions

A functional prototype of an RBP was 3D-printed to demonstrate the effectiveness of all-in-one 3D printing with magnetic materials for rapid prototyping. The presented method allows for the integration of arbitrarily-shaped permanent magnets in a single print. In comparison with similar research, our polymer-bonded magnetic filament was able to be printed from a standard spool without breaking and is processable on a low-cost Bowden style printer. Furthermore, compared to current magnetic FDM prints, slightly higher remanences were achieved.

Beyond the presented case of blood pump development, 3D printing of integrated magnets allows for an increase of design complexity at low costs early in product development, and contributes to speeding up the development process of medical devices.

**Author Contributions:** K.v.P.-C. conceived the idea, designed the experiments and wrote the paper, Y.H. fabricated the filament and prototype, J.C. performed SEM and TGA., A.H. performed the magnetization and permagraph measurements; S.B. contributed to the pump design and testing, D.P. contributed materials and tools; M.S.D. and M.M. supervised the work, all contributed to the writing of this manuscript.

**Funding:** This research received no external funding.

**Acknowledgments:** Infrastructures of the Arnold Magnetic Technologies AG, Lupfig, Switzerland and the ZHAW Zurich University of Applied Sciences, Winterthur, Switzerland were used. This work is part of the Zurich Heart project under the umbrella of University Medicine Zurich.

**Conflicts of Interest:** The authors declare no conflict of interest.

#### References

1. Brown, D.; Ma, B.-M.; Chen, Z. Developments in the processing and properties of NdFeB-type permanent magnets. *J. Magn. Magn. Mater.* **2002**, *248*, 432–440. [[CrossRef](#)]
2. Li, L.; Tirado, A.; Nlebedim, I.C.; Rios, O.; Post, B.; Kunc, V.; Lowden, R.R.; Lara-Curzio, E.; Fredette, R.; Ormerod, J.; et al. Big Area Additive Manufacturing of High Performance Bonded NdFeB Magnets. *Sci. Rep.* **2016**, *6*. [[CrossRef](#)] [[PubMed](#)]
3. Huber, C.; Abert, C.; Bruckner, F.; Groenefeld, M.; Muthsam, O.; Schuschnigg, S.; Sirak, K.; Thanhoffer, R.; Teliban, I.; Vogler, C.; et al. 3D print of polymer bonded rare-earth magnets, and 3D magnetic field scanning with an end-user 3D printer. *Appl. Phys. Lett.* **2016**, *109*, 162401. [[CrossRef](#)]



4. Huber, C.; Abert, C.; Bruckner, F.; Pfaff, C.; Kriwet, J.; Groenefeld, M.; Teliban, I.; Vogler, C.; Suess, D. Topology optimized and 3D printed polymer-bonded permanent magnets for a predefined external field. *J. Appl. Phys.* **2017**, *122*, 053904. [[CrossRef](#)]
5. Huber, C.; Abert, C.; Bruckner, F.; Groenefeld, M.; Schuschnigg, S.; Teliban, I.; Vogler, C.; Wautischer, G.; Windl, R.; Suess, D. 3D Printing of Polymer-Bonded Rare-Earth Magnets With a Variable Magnetic Compound Fraction for a Predefined Stray Field. *Sci. Rep.* **2017**, *7*. [[CrossRef](#)] [[PubMed](#)]
6. Jaćimović, J.; Binda, F.; Herrmann, L.G.; Greuter, F.; Genta, J.; Calvo, M.; Tomše, T.; Simon, R.A. Net Shape 3D Printed NdFeB Permanent Magnet: Net Shape 3D Printed NdFeB Permanent Magnet. *Adv. Eng. Mater.* **2017**, *19*, 1700098. [[CrossRef](#)]
7. Paranthaman, M.P.; Shafer, C.S.; Elliott, A.M.; Siddel, D.H.; McGuire, M.A.; Springfield, R.M.; Martin, J.; Fredette, R.; Ormerod, J. Binder Jetting: A Novel NdFeB Bonded Magnet Fabrication Process. *JOM* **2016**, *68*, 1978–1982. [[CrossRef](#)]
8. Yan, Y.; Liu, L.; Ding, C.; Nguyen, L.; Moss, J.; Mei, Y.; Lu, G.Q. Additive Manufacturing of Magnetic Components for Heterogeneous Integration. In Proceedings of the 2017 IEEE 67th Electronic Components and Technology Conference (ECTC), Lake Buena Vista, FL, USA, 30 May–2 June 2017; pp. 324–330.
9. Compton, B.G.; Kemp, J.W.; Novikov, T.V.; Pack, R.C.; Nlebedim, C.I.; Duty, C.E.; Rios, O.; Paranthaman, M.P. Direct-write 3D printing of NdFeB bonded magnets. *Mater. Manuf. Process.* **2018**, *33*, 109–113. [[CrossRef](#)]
10. Li, L.; Jones, K.; Sales, B.; Pries, J.L.; Nlebedim, I.C.; Jin, K.; Bei, H.; Post, B.K.; Kesler, M.S.; Rios, O.; et al. Fabrication of highly dense isotropic Nd-Fe-B nylon bonded magnets via extrusion-based additive manufacturing. *Addit. Manuf.* **2018**, *21*, 495–500. [[CrossRef](#)]
11. Schumer, E.M.; Black, M.C.; Monreal, G.; Slaughter, M.S. Left ventricular assist devices: Current controversies and future directions. *Eur. Heart J.* **2016**, *37*, 3434–3439. [[CrossRef](#)] [[PubMed](#)]
12. Schmid Daners, M.; Kaufmann, F.; Amacher, R.; Ochsner, G.; Wilhelm, M.J.; Ferrari, A.; Mazza, E.; Poulikakos, D.; Meboldt, M.; Falk, V. Left Ventricular Assist Devices: Challenges Toward Sustaining Long-Term Patient Care. *Ann. Biomed. Eng.* **2017**, *45*, 1836–1851. [[CrossRef](#)] [[PubMed](#)]
13. Wiegmann, L.; Boës, S.; de Zélicourt, D.; Thamsen, B.; Schmid Daners, M.; Meboldt, M.; Kurtcuoglu, V. Blood Pump Design Variations and Their Influence on Hydraulic Performance and Indicators of Hemocompatibility. *Ann. Biomed. Eng.* **2018**, *46*, 417–428. [[CrossRef](#)] [[PubMed](#)]
14. Nishida, M.; Negishi, T.; Sakota, D.; Kosaka, R.; Maruyama, O.; Hyakutake, T.; Kuwana, K.; Yamane, T. Properties of a monopivot centrifugal blood pump manufactured by 3D printing. *J. Artif. Organs* **2016**, *19*, 322–329. [[CrossRef](#)] [[PubMed](#)]
15. Throckmorton, A.L.; Kapadia, J.Y.; Chopski, S.G.; Bhavsar, S.S.; Moskowitz, W.B.; Gullquist, S.D.; Gangemi, J.J.; Haggerty, C.M.; Yoganathan, A.P. Numerical, Hydraulic, and Hemolytic Evaluation of an Intravascular Axial Flow Blood Pump to Mechanically Support Fontan Patients. *Ann. Biomed. Eng.* **2011**, *39*, 324–336. [[CrossRef](#)] [[PubMed](#)]
16. Chan, W.K.; Wong, Y.W.; Chua, C.K.; Lee, C.W.; Feng, C. Rapid manufacturing techniques in the development of an axial blood pump impeller. *Proc. Inst. Mech. Eng.* **2003**, *217*, 469–475. [[CrossRef](#)] [[PubMed](#)]
17. Lalehpour, A.; Barari, A. Post processing for Fused Deposition Modeling Parts with Acetone Vapour Bath. *IFAC-Pap.* **2016**, *49*, 42–48. [[CrossRef](#)]
18. Garg, A.; Bhattacharya, A.; Batish, A. Chemical vapor treatment of ABS parts built by FDM: Analysis of surface finish and mechanical strength. *Int. J. Adv. Manuf. Technol.* **2017**, *89*, 2175–2191. [[CrossRef](#)]
19. Galantucci, L.M.; Lavecchia, F.; Percoco, G. Experimental study aiming to enhance the surface finish of fused deposition modeled parts. *CIRP Ann.* **2009**, *58*, 189–192. [[CrossRef](#)]
20. Alsoufi, M.S.; Elsayed, A.E. Surface Roughness Quality and Dimensional Accuracy—A Comprehensive Analysis of 100% Infill Printed Parts Fabricated by a Personal/Desktop Cost-Effective FDM 3D Printer. *Mater. Sci. Appl.* **2018**, *9*, 11–40. [[CrossRef](#)]
21. VACODYM-VACUUMSCHMELZE GmbH & Co. KG. Available online: <https://www.vacuumschmelze.de/de/produkte/dauermagnete-systeme/dauermagnete/nd-fe-b/vacodym.html> (accessed on 10 July 2018).
22. Magnetfabrik Bonn. Produkte:: Magnete nach Formgebung:: Spritzguss. Available online: [https://www.magnetfabrik.de/magnetfabrik\\_de/produkte.php?category=12&page=606](https://www.magnetfabrik.de/magnetfabrik_de/produkte.php?category=12&page=606) (accessed on 10 July 2018).

23. Linneweber, J.; Dohmen, P.M.; Kerzschner, U.; Affeld, K.; Nosé, Y.; Konertz, W. The Effect of Surface Roughness on Activation of the Coagulation System and Platelet Adhesion in Rotary Blood Pumps. *Artif. Organs* **2007**, *31*, 345–351. [[CrossRef](#)] [[PubMed](#)]
24. Kim, Y.; Yuk, H.; Zhao, R.; Chester, S.A.; Zhao, X. Printing ferromagnetic domains for untethered fast-transforming soft materials. *Nature* **2018**, *558*, 274. [[CrossRef](#)] [[PubMed](#)]



© 2018 by the authors. Licensee MDPI, Basel, Switzerland. This article is an open access article distributed under the terms and conditions of the Creative Commons Attribution (CC BY) license (<http://creativecommons.org/licenses/by/4.0/>).